JACC: BASIC TO TRANSLATIONAL SCIENCE VOL. 8, NO. 8, 2023

ORIGINAL RESEARCH - PRECLINICAL

IFN-γ-STAT1-ERK Pathway Mediates Protective Effects of Invariant Natural Killer T Cells Against Doxorubicin-Induced Cardiomyocyte Death

Masashi Sada, MD,[a,b] Shouji Matsushima, MD, PhD,[a,b] Masataka Ikeda, MD, PhD,[a,b] Soichiro Ikeda, MD, PhD,[a,b] Kosuke Okabe, MD, PhD,[a,b] Akihito Ishikita, MD, PhD,[a,b] Tomonori Tadokoro, MD, PhD,[a,b] Nobuyuki Enzan, MD, PhD,[a,b] Taishi Yamamoto, MD,[a,b] Hiroko Deguchi Miyamoto, MD, PhD,[a,b] Yoshitomo Tsutsui, MD,[a,b] Ryo Miyake, MD,[a,b] Daiki Setoyama, PhD,[c] Dongchon Kang, MD, PhD,[c] Tomomi Ide, MD, PhD,[a] Hiroyuki Tsutsui, MD, PhD[a,b]

VISUAL ABSTRACT

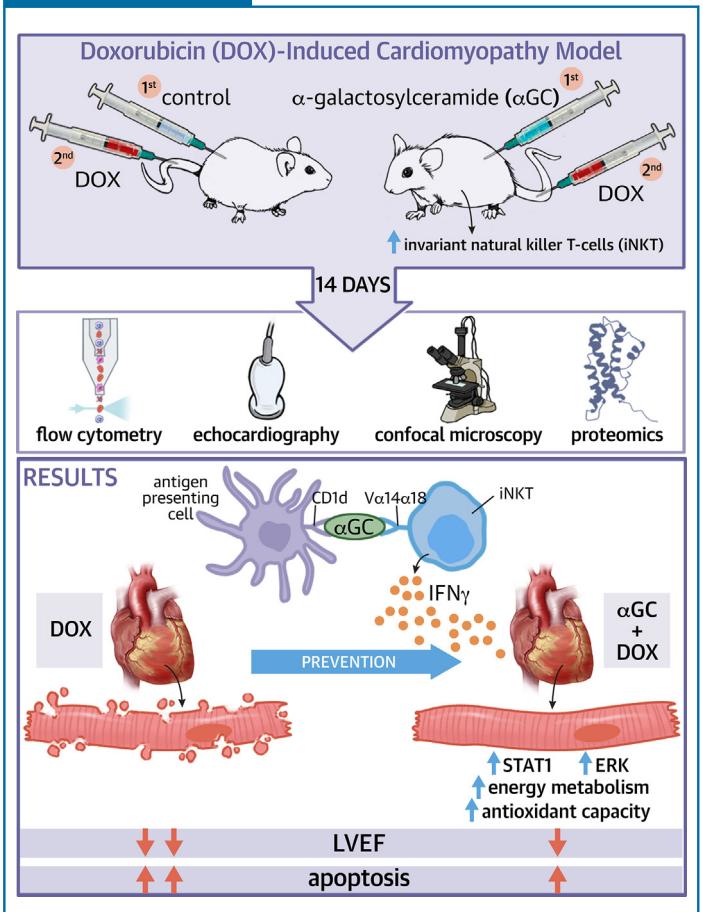

Sada M, et al. J Am Coll Cardiol Basic Trans Science. 2023;8(8):992-1007.

HIGHLIGHTS

- **DOX-induced cardiomyopathy has poor prognosis. Myocardial inflammation is involved in the pathophysiology of DOX-induced cardiomyopathy.**
- **Activation of iNKT cells is known to exert protective effects against myocardial cell death by regulating inflammatory cytokines.**
- **Activation of iNKT cells by αGC attenuated DOX-induced cardiomyocyte death and cardiac dysfunction.**
- **Mass spectrometric analysis exhibited that αGC preserved 50 energy metabolism and redox-related proteins in DOX-treated hearts.**
- **IFN-γ-STAT1-ERK pathway mediates the beneficial effects of activation of NKT cells in DOX-induced cardiomyopathy.**

ISSN 2452-302X https://doi.org/10.1016/j.jacbts.2023.02.014

SUMMARY

Doxorubicin (DOX)-induced cardiomyopathy has poor prognosis, and myocardial inflammation is intimately involved in its pathophysiology. The role of invariant natural killer T (iNKT) cells has not been fully determined in this disease. We here demonstrated that activation of iNKT cells by α-galactosylceramide (GC) attenuated DOX-induced cardiomyocyte death and cardiac dysfunction. αGC increased interferon (IFN)-γ and phosphorylation of signal transducers and activators of transcription 1 (STAT1) and extracellular signal-regulated kinase (ERK). Administration of anti-IFN-γ neutralizing antibody abrogated the beneficial effects of αGC on DOX-induced cardiac dysfunction. These findings emphasize the protective role of iNKT cells in DOX-induced cardiomyopathy via the IFN-γ-STAT1-ERK pathway. (J Am Coll Cardiol Basic Trans Science 2023;8:992–1007)

ABBREVIATIONS AND ACRONYMS

Bax = Bcl-2-associated X protein
Bcl-2 = B cell/CLL lymphoma 2
BW = body weight
DOX = doxorubicin
ERK = extracellular signal-regulated kinase
FAO = fatty acid oxidation
GC = galactosylceramide
IFN = interferon
IL = interleukin
IP = intraperitoneal
LV = left ventricular
LVDd = left ventricular diastolic diameter
LVDs = left ventricular systolic diameter
LVEF = left ventricular ejection fraction
iNKT = invariant natural killer T
NF-κB = nuclear factor-kappa B
STAT1 = signal transducers and activators of transcription 1
TCA = tricarboxylic acid
TNF = tumor necrosis factor
TUNEL = terminal deoxynucleotidyl transferase dUTP nick end labeling

Doxorubicin (DOX), an anthracycline antibiotic, is a widely used and efficacious chemotherapeutic drug for hematological malignancies and solid tumors; however, it has dose-dependent cardiotoxicity, such as cardiomyocyte death and cardiac dysfunction, thereby limiting its clinical use.[1] DOX-induced cardiomyopathy has poor prognosis compared with dilated or ischemic cardiomyopathy.[2] Therefore, the establishment of effective therapeutic strategy for DOX-induced cardiomyopathy is urgently needed.

Cardiomyocyte death, such as apoptosis, is a critical process implicated in DOX-induced cardiomyopathy.[3-5] A number of studies have suggested the molecular mechanisms of this disease state, including alteration of transcription by topoisomerase II,[6] mitochondrial iron accumulation,[7] abnormalities of energy metabolism such as the tricarboxylic acid (TCA) cycle,[8] fatty acid oxidation (FAO),[9] mitochondrial oxidative phosphorylation,[10] and oxidative stress.[11,12] In addition to these factors, inflammation is known to be intimately involved in DOX-induced cardiomyopathy. DOX increased systemic interleukin (IL)-1β levels through activation of nucleotide-binding oligomerization domain, leucine rich repeat and pyrin domain containing proteins (NLRP3) inflammasome.[13] IL-1β, IL-6, and tumor necrosis factor (TNF)-α were increased in DOX-treated H9C2 cells and inhibition of nuclear factor-kappa B (NF-κB) attenuated DOX-induced cardiac injury by decreasing the levels of these cytokines.[14] A deficiency of toll like receptor 4 (TLR4), a part of the innate immune system, attenuated DOX-induced cardiac apoptosis by suppressing TNF-α expression.[15] Recently, exosome treatment has been reported to play a protective role in DOX-induced cardiomyopathy by increasing IL-10.[16] These findings indicate that inflammatory cytokines are involved in the pathophysiology of DOX-induced cardiomyopathy and could be its potential therapeutic targets.

Invariant natural killer T (iNKT) cells are an innate-like T-lymphocyte population coexpressing NK markers and an αβ T cell receptor that recognizes glycolipid antigens. They can rapidly and robustly produce a mixture of T-helper type 1 (Th1) and type 2 (Th2) cytokines, such as interferon (IFN)-γ, TNF-α, IL-4, and IL-10, and orchestrate tissue inflammation in cardiovascular diseases.[17] iNKT cells have been demonstrated to play a protective role in myocardial apoptosis in the left ventricular (LV) remodeling and ischemia-reperfusion injury by increasing IL-10.[18,19] More recently, activation of iNKT cells attenuated cardiac fibrosis in DOX-treated mice by upregulating Th2 cytokines.[20] These findings suggest that iNKT cells may have beneficial effects on cardiac dysfunction via regulating cytokines; however, no previous studies have clarified the effects of iNKT cells on cardiomyocyte death in DOX-

From the [a]Department of Cardiovascular Medicine, Faculty of Medical Sciences, Kyushu University, Fukuoka, Japan; [b]Division of Cardiovascular Medicine, Research Institute of Angiocardiology, Faculty of Medical Sciences, Kyushu University, Fukuoka, Japan; and the [c]Department of Clinical Chemistry and Laboratory Medicine, Graduate School of Medical Sciences, Kyushu University, Fukuoka, Japan.
The authors attest they are in compliance with human studies committees and animal welfare regulations of the authors' institutions and Food and Drug Administration guidelines, including patient consent where appropriate. For more information, visit the Author Center.

Manuscript received January 26, 2022; revised manuscript received February 24, 2023, accepted February 25, 2023.

induced cardiomyopathy. Moreover, the molecular mechanism of beneficial effects of iNKT cells in the disease state has not been fully elucidated.

Therefore, the aims of this study were to determine whether activation of iNKT cells by α-galactosylceramide (αGC), a specific activator for iNKT cells, could attenuate DOX-induced cardiomyocyte death and cardiomyopathy and, if so, to elucidate its molecular mechanism.

METHODS

DOXORUBICIN-INDUCED CARDIOMYOPATHY MODEL. C57BL/6J mice were purchased from Kyudo Co, Ltd. Animals were used for experiments at 9 to 10 weeks of age (weight 22-26 g). Mice were bred in a pathogen-free environment, provided standard chow diet and water, and kept under a constant 12-hour light-dark cycle at a temperature of 23 to 25 °C. Mice received an intraperitoneal (IP) injection of either αGC (0.1 μg/g; Funakoshi Co, Ltd) or phosphate-buffered saline. After 1 week, these mice were treated with DOX (18 mg/kg via 3 intravenous injections over 1 week; Sigma-Aldrich) or distilled water, as described previously,[21] and were followed for 14 days. Gene expression levels of various cytokines were evaluated 7 days and 14 days after the first injection of DOX (Supplemental Figure 1A). Furthermore, to examine the role of IFN-γ in the effects of αGC on DOX-induced cardiomyopathy, rat anti-IFN-γ monoclonal antibody (100 μg/mouse, IP; BioLegend) or rat immunoglobulin G1 isotype control (100 μg/mouse, IP; R&D Systems, Inc) was administered 7 days after the first injection of DOX (Supplemental Figure 1B).

All procedures involving animals and animal care protocols were approved by the Committee on Ethics of Animal Experiments of the Kyushu University Graduate School of Medicine and Pharmaceutical Sciences and were performed in accordance with the Guideline for Animal Experiments of Kyushu University.

ECHOCARDIOGRAPHY. Under light anesthesia with 1% to 2% isoflurane, 2-dimensional targeted M-mode images were obtained from the short axis view at the papillary muscle level using a Vevo 2100 ultrasonography system (Visual Sonics), as previously described.[22] Left ventricular ejection fraction (LVEF) was calculated by the following formula that was pre-programmed in the system: LVEF = [(diastolic LV volume − systolic LV volume) / diastolic LV volume) × 100], where LV volume = [(7.0 / (2.4 + LV diameter)] × LV diameter.[3]

HISTOLOGICAL ANALYSES. LV accompanied by the septum was cut into base and apex portions, fixed with 10% formalin, and submitted for hematoxylin and eosin staining. Collagen volume was determined by quantitative morphometry of tissue sections from the mid-LV stained with Masson's trichrome as described previously.[23] LV sections were immunostained with antibody against mouse CD3 (a T cell marker) or Mac3 (a macrophage marker), followed by counterstaining with hematoxylin.

TUNEL STAINING. Terminal deoxynucleotidyl transferase dUTP nick end labeling (TUNEL) staining was conducted as described.[24] Deparaffinized sections were incubated with proteinase K and DNA fragments were labeled with fluorescein-conjugated dUTP using in situ Apoptosis Detection kit (MK500, Takara). Nuclear density was determined by manual counting of 4′,6-diamidino-2-phenylindole (DAPI)-stained nuclei in 10 fields for each animal using a ×40 objective.

IMMUNOBLOT ANALYSES. Heart homogenates and cardiomyocyte lysates were prepared in RIPA lysis buffer containing Tris-HCl, NaCl, NP-40, sodium deoxycholate, and sodium dodecyl sulfate. For immunoblot analyses, we used primary antibodies from Cell Signaling Technology and Abcam against the following proteins: Bcl-2-associated X protein (Bax) (CST #4436), B cell/CLL lymphoma 2 (Bcl-2) (CST #8242), cleaved caspase 3 (CST #9664), phosphorylation of signal transducers and activators of transcription 1 (p-STAT1) (CST #7649), signal transducers and activators of transcription 1 (STAT1) (CST #14995), phosphorylation of extracellular signal-regulated kinase (p-ERK) (CST #9109), extracellular signal-regulated kinase (ERK) (CST #9102), p-Akt (Ser473) (CST #4060), Akt (CST #9272), phospho-JNK (p-JNK) (CST #4668), c-Jun N-terminal kinase (JNK) (CST #9258), p-p38 (CST #4511), p38 (CST #9212), and p-MLKL (ab196436). GAPDH (sc32233, Santa Cruz Biotechnology) was used as a loading control.

QUANTITATIVE REAL-TIME POLYMERASE CHAIN REACTION. Methods of quantitative real-time polymerase chain reaction have been described previously.[25] In brief, after preparing total RNA, first-strand cDNA was synthesized. Real-time polymerase chain reaction was then carried out on QuantStudio 3 (Thermo Fisher Scientific) using the THUNDERBIRD SYBR qPCR Mix (TOYOBO). The specific oligonucleotide primers for *Rps18*, *Vα14Jα18*, *Il1b*, *Il4*, *Il6*, *Il10*, *Tnfa*, *Ifng*, *Cd11c*, *Arg1*, *Mcp1*, and *Rantes* were selected using Perfect Real Time Primer. The oligonucleotide primers were as follows: *Rps18*, sense 5′-TTCTGGCCAACGGTCTAGACAAC-3′ and antisense

5′-CCAGTGGTCTTGGTGTGCTGA-3′; *Vα14Jα18*, sense 5′-CTAAGCACAGCACGCTGCACA-3′ and antisense 5′-CAAAATGCAGCCTCCCTAAG-3′; *Il1b*, sense 5′-TCCAGGATGAGGACATGAGCAC-3′ and antisense 5′-GAACGTCACACACCAGCAGGTTA-3′; *Il4*, sense 5′-ACGGAGATGGATGTGCCAAAC-3′ and antisense 5′-AGCACCTTGGAAGCCCTACAGA-3′; *Il6*, sense 5′-CCACTTCACAAGTCGGAGGCTTA-3′ and antisense 5′-GCAAGTGCATCATCGTTGTTCATAC-3′; *IL10*, sense 5′-GCCAGAGCCACATGCTCCTA-3′ and antisense 5′-GATAAGGCTTGGCAACCCAAGTAA-3′; *Tnfa*, sense 5′- AAGCCTGTAGCCCACGTCGTA-3′ and antisense 5′-GGCACCACTAGTTGGTTGTCTTTG-3′; *Ifng*, sense 5′-TACACACTGCATCTTGGCTTTG-3′ and antisense 5′-CTTCCACATCTATGCCACTTGAG-3′, *Cd11c*, sense 5′-TATCGTGGGCAGCTCAGTGG-3′ and antisense 5′-GCGGGTTCAAAGACGATGG-3′, *Arg1*, sense 5′-AGCTCTGGGAATCTGCATGG-3′ and antisense 5′-ATGTACACGATGTCTTTGGCAGAT-3′, *Mcp1*, sense 5′-AGCAGCAGGTGTCCCAAAGA-3′ and antisense 5′-GTGCTGAAGACCTTAGGGCAGA-3′, *Rantes*, sense 5′-ACCAGCAGCAAGTGCTCCAA-3′ and antisense 5′-TGGCTAGGACTAGAGCAAGCAATG-3′. These transcripts were normalized to *Rps18*.

FLOW CYTOMETRY. LV tissues were harvested, minced with a fine scissors, placed in 4 mL RPMI-1640 (Thermo Fisher Scientific) with 5% fetal bovine serum, 450 U/mL collagenase type I, 125 U/mL collagenase type XI, 60 U/mL DNase I, and 60 U/mL hyaluronidase (all from Sigma-Aldrich), and shaken at 37 °C for 40 minutes. Tissues were then triturated through 70-μm nylon mesh and centrifuged (1,000 rpm, 5 minutes, 4 °C). Cells were incubated with anti-CD16/32 monoclonal antibody (BD Pharmingen) to block nonspecific binding of primary monoclonal antibody and then stained with a combination of allophycocyanin conjugated anti-mouse CD45 (BD Pharmingen), fluorescein isothiocyanate conjugated anti-mouse TCRβ (BD Pharmingen), and phycoerythrin conjugated αGC-loaded murine CD1d tetramer (MBL International) for 1 hour at 4°C. Cells were washed, and 7-Amino-Actinomycin D (Immunostep) was added to distinguish dead cells. αGC-loaded CD1d tetramer$^+$ TCRβ$^+$ cells were identified as iNKT cells. Stained cells were acquired with FACSVerse flow cytometer (BD Biosciences) and analyzed with FlowJo (Tommy Digital Biology).

LIQUID CHROMATOGRAPHY-MASS SPECTROMETRY ANALYSIS. Detailed methods are available in the Supplemental Methods. The mass spectrometry proteomics data are available from ProteomeXchange and Japan ProteOme STandard Repository/Database (jPOST). The accession numbers are PXD031182 for ProteomeXchange and JPST001457 for jPOST, respectively.

STATISTICAL ANALYSIS. All values are expressed as mean ± SEM. Normality of data was confirmed by Shapiro-Wilk test. Comparisons between 2 groups were performed using Student's *t*-test, while comparisons among more than 2 groups were conducted using analysis of variance with Tukey's post hoc test or Kruskal-Wallis test for multiple pairwise comparisons. Survival over 14 days is presented using Kaplan-Meier methods and compared using the log-rank test. A P value of <0.05 was considered statistically significant. GraphPad Prism 9 software (GraphPad Software) was used for statistical analyses.

RESULTS

αGC ADMINISTRATION ACTIVATED iNKT CELLS IN DOX-TREATED HEARTS. First, we evaluated the effect of αGC on iNKT cells in DOX-treated hearts. αGC significantly increased gene expression of Vα14Jα18, a marker of iNKT cells, in hearts treated with and without DOX at day 7 and day 14 (Figure 1A). Flow cytometric analysis demonstrated that αGC tended to increase the number of iNKT cells and significantly increased their proportion in hearts treated with and without DOX at day 14 (Figure 1B). These data suggest that αGC significantly activates iNKT cells in DOX-treated hearts.

αGC ADMINISTRATION ATTENUATED DOX-INDUCED CARDIAC DYSFUNCTION. DOX decreased body weight (BW) and αGC prevented DOX-induced BW loss (Figure 2A). DOX and αGC did not alter heart rate and systolic blood pressure (Figure 2B). DOX increased left ventricular systolic diameter (LVDs) and decreased LVEF (Figure 2C) and αGC attenuated these changes (Figure 2C). It also ameliorated DOX-induced decreases in whole heart and LV weights (Figure 2D). These data indicate that activation of iNKT cells attenuates DOX-induced cardiac dysfunction.

αGC ADMINISTRATION ATTENUATED DOX-INDUCED CARDIOMYOCYTE INJURY AND APOPTOSIS. αGC ameliorated DOX-induced cardiomyocyte injury evaluated by number of cytoplasmic vacuolizations (Figure 3A). It also suppressed DOX-induced myocardial apoptosis evaluated by TUNEL staining (Figure 3B). The ratio of Bax, an apoptotic factor, to Bcl-2, an anti-apoptotic factor, and cleaved caspase 3, a marker of apoptosis, were increased in DOX-treated mice, and αGC significantly decreased it (Figures 3C and 3D). On the other hand, DOX did not increase phosphorylation of MLKL, a marker of necroptosis,

FIGURE 1 αGC Administration Activated iNKT Cells in DOX-Treated Hearts

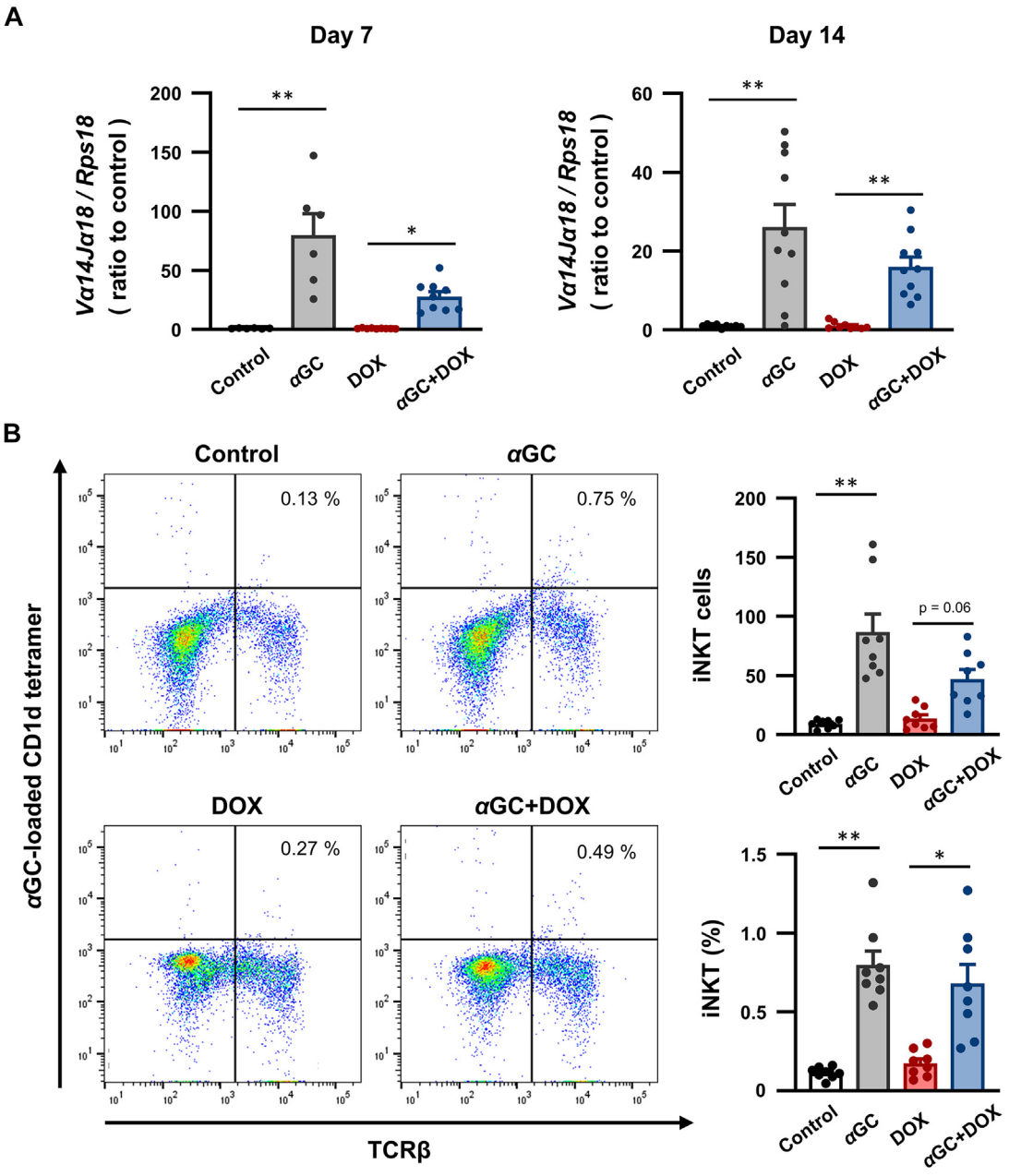

(A) Gene expression of *Vα14Jα18* in the left ventricle (LV) of vehicle and α-galactosylceramide (αGC)-treated mice 7 days and 14 days after doxorubicin (DOX) injection (n = 10). They were normalized to *Rps18* gene expression and expressed as ratio to control group. **(B)** Representative flow cytometric assessment of cardiac mononuclear cells obtained from the LV of vehicle and αGC-treated mice 14 days after DOX injection. Cardiac mononuclear cells from 8 different mice for each group were pooled and analyzed. αGC-loaded CD1d tetramer$^+$ TCRβ$^+$ cells were identified as invariant natural killer T (iNKT) cells. The inset numbers are a percentage of the gated region of the samples. Summary data for the number and proportion of iNKT cells. Data are expressed as mean ± SEM. *$P < 0.05$, **$P < 0.01$: analysis of variance (ANOVA) with Tukey's post hoc test or Kruskal-Wallis test.

and αGC did not change it in DOX-treated mice (Supplemental Figure 2). We also evaluated collagen volume fraction, an index of interstitial fibrosis. αGC did not affect DOX-induced increases in collagen volume fraction in the heart (Supplemental Figure 3). We also evaluated interstitial fibrosis 28 days after DOX treatment. αGC tended to suppress it but the effect was not significant (Supplemental Figure 4). These findings indicate that the suppression of myocardial injury and apoptosis mediates protective effects of iNKT cells in DOX-induced cardiac dysfunction.

αGC ADMINISTRATION DID NOT AFFECT INFILTRATION OF INFLAMMATORY CELLS IN DOX-TREATED HEARTS. Immunohistochemical analysis revealed that DOX increased the number of CD3 (as a marker of T-lymphocyte)-positive cells but αGC did not change it (Supplemental Figure 5A). αGC did not affect the number of Mac3 (as a marker of macrophage)-positive cells in DOX-treated mice (Supplemental Figure 5B). We also investigated whether αGC could affect leukocytes, macrophages, and their subtypes (M1 and M2) in the heart by flow cytometric analysis (Supplemental Figure 6A). αGC did not affect the number and proportion of leukocytes in DOX-treated mice (Supplemental Figure 6B). Although DOX increased the number and proportion of total macrophages, the number of M1 macrophages, and decreased the proportion of M2 macrophages, αGC did not change them (Supplemental Figures 6C to 6E). Furthermore, it did not affect expression levels of CD11c (as a marker of M1 macrophages), arginase 1 (Arg-1) (as a marker of M2 macrophages), monocyte chemoattractant protein (MCP)-1, and regulated on activation, normal T cell expressed and secreted (RANTES) (Supplemental Figure 7).

αGC ADMINISTRATION INCREASED IFN-γ PRODUCTION IN DOX-TREATED HEARTS. To further investigate the mechanism mediating cardioprotective effects by activation of iNKT cells on DOX-induced cardiomyopathy, we evaluated the myocardial gene expression of various cytokines at day 7 and day 14. Although DOX increased IL-1β and IL-6 at day 14, αGC did not affect them (**Figures 4A and 4B**). DOX did not change TNF-α, IL-4, and IL-10, and αGC did not affect them in DOX-treated mice (**Figures 4C to 4E**). In contrast, αGC increased IFN-γ both at day 7 and day 14 in DOX-treated hearts (**Figure 4F**). These data suggest that IFN-γ is a predominant cytokine persistently increased by activation of iNKT cells in DOX-treated mice.

αGC ADMINISTRATION INCREASED PHOSPHORYLATION OF STAT1, ERK, AND AKT IN DOX-TREATED HEARTS. Next, we evaluated the downstream targets of IFN-γ. Consistent with IFN-γ, αGC increased total protein level and phosphorylation of signal transducers and activators of transcription 1 (STAT1), a direct downstream of IFN-γ receptor, in hearts treated with and without DOX (**Figures 5A and 5B**). STAT1 is known to regulate survival pathway, including mitogen-activated protein (MAP) kinases and Akt. Among these proteins, αGC increased phosphorylation of ERK and Akt, but not JNK or p38, in DOX-treated hearts (**Figure 5B**). These data indicate that STAT1-ERK/Akt axis might be involved in protective effects of iNKT cells in DOX-induced cardiomyopathy.

αGC ADMINISTRATION PREVENTED DECREASES IN ENERGY METABOLISM AND REDOX-RELATED PROTEINS IN DOX-TREATED HEARTS. Energy metabolism and oxidative stress are intimately involved in cardiomyocyte death. To evaluate the impact of activated iNKT cells by αGC on energy metabolism and oxidative stress in DOX-induced cardiomyopathy, we performed mass spectrometry in control, DOX-treated, and DOX + αGC-treated hearts to obtain global protein profiles. We detected 798 proteins as a whole. Among them, the score of 131 proteins, which was calculated on the basis of XCorr value for peptide spectrum matches by the Sequest HT search engine and suggested to approximate the amount of protein in some extent, were decreased in DOX-treated hearts and preserved by αGC (Supplemental Table 1). These proteins contained 26 oxidative phosphorylation-related proteins such as NDUFA4, NDUFA7, and NDUFA10 (Supplemental Figure 8A); 8 TCA cycle-related proteins such as MDH1, SDHB, and IDH3A (Supplemental Figure 8B); 11 FAO-related proteins such as ACSL1, CPT2, and ACADM (Supplemental Figure 8C); and 5 antioxidant capacity-related proteins such as SOD2, Prdx1, and Prdx5 (Supplemental Figure 8D). These data suggest that activation of iNKT cells by αGC contributes to preserve proteins related to energy metabolism and antioxidant capacity in DOX-induced cardiomyopathy.

NEUTRALIZATION OF IFN-γ ABOLISHED PROTECTIVE EFFECTS OF αGC ON DOX-INDUCED CARDIAC DYSFUNCTION AND APOPTOSIS. To elucidate the role of IFN-γ in protective effects of iNKT cells on DOX-induced cardiomyopathy, we administrated neutralizing anti-IFN-γ monoclonal antibody into mice treated with only DOX or with αGC and DOX. Administration of anti-IFN-γ antibody affected neither left ventricular diastolic diameter (LVDd), LVDs, nor LVEF in DOX-treated mice (**Figure 6A**). In addition, it did not change myocardial apoptosis evaluated by TUNEL staining (**Figure 6B**), Bax to Bcl-2 ratio (**Figure 6C**), and cleaved caspase 3 (**Figure 6D**) in

FIGURE 2 αGC Administration Attenuated DOX-Induced Cardiac Dysfunction

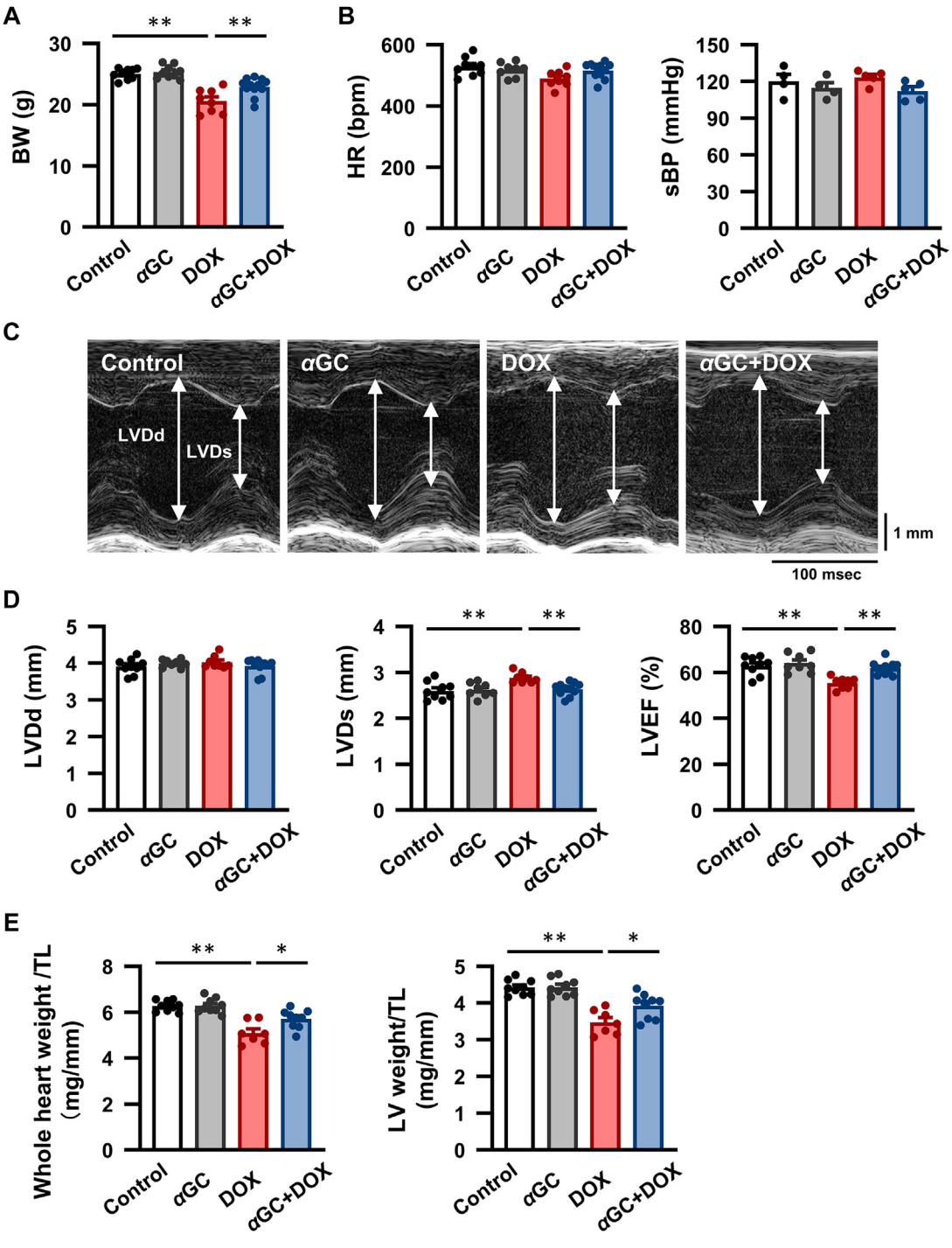

(A and B) Body weight (BW), heart rate (HR), and systolic blood pressure (sBP) in vehicle and αGC-treated mice 14 days after DOX injection (n = 8-12). **(C)** Representative echocardiographic images and left ventricular end-diastolic diameter (LVDd), left ventricular end-systolic diameter (LVDs), and left ventricular ejection fraction (LVEF) in the indicated groups (n = 8-11). **(D)** Whole heart weight to tibial length (TL) and LV weight to TL ratio in the indicated groups (n = 9). Data are expressed as mean ± SEM. *$P < 0.05$, **$P < 0.01$: ANOVA with Tukey's post hoc test or Kruskal-Wallis test. Abbreviations as in Figure 1.

DOX-treated mice. Consistently, phosphorylation of STAT1, ERK, and Akt in DOX-treated hearts was not changed by administration of anti-IFN-γ antibody at day 8 (**Figure 6E**) and day 14 (Supplemental Figure 9). On the other hand, anti-IFN-γ antibody did not change LVDd (**Figure 6A**) but tended to increase LVDs and significantly decrease LVEF in mice treated with αGC and DOX (**Figure 6A**). Furthermore, anti-IFN-γ antibody increased myocardial apoptosis evaluated by TUNEL staining (**Figure 6B**), ratio of Bax to Bcl-2 (**Figure 6C**), and cleaved caspase 3 (**Figure 6D**) in mice treated with αGC and DOX, which was accompanied by suppression of phosphorylation of ERK, but not Akt (**Figure 6D**, Supplemental Figure 9). These findings indicate that activation of iNKT cells could exert protective effects in DOX-induced cardiomyopathy via the IFN-γ-STAT1-ERK pathway.

PRE-ADMINISTRATION OF αGC WAS ASSOCIATED WITH ITS PROTECTIVE EFFECTS AGAINST DOX-INDUCED CARDIAC DYSFUNCTION. We further investigated the role of iNKT cells in DOX-induced cardiac dysfunction in 2 other protocols. Additional protocol 1 was simultaneous administration of αGC and DOX (Supplemental Figure 10A). In this protocol, αGC did not ameliorate DOX-induced decreases in BW, LV weight (Supplemental Figure 10B), and LVEF (Supplemental Figure 10C). αGC did not increase IFN-γ production in DOX-treated hearts (Supplemental Figure 11). Furthermore, it did not increase phosphorylation of STAT1 and ERK (Supplemental Figure 12A) and suppress ratio of Bax to Bcl-2 (Supplemental Figure 12B) in DOX-treated hearts. These data suggest that simultaneous administration of αGC and DOX did not efficiently exert beneficial effects in DOX-treated hearts.

To investigate whether IFN-γ-STAT1-ERK pathway mediates beneficial effects of activation of iNKT cells in a previously reported model,[20] we conducted additional protocol 2, which was administration of αGC before and after a single DOX injection (Supplemental Figure 13A). In this protocol, αGC significantly improved DOX-induced decreases in BW and LV weight (Supplemental Figure 13B) and LVEF (Supplemental Figure 13C). In addition, αGC prevented DOX-induced death for 14 days (Supplemental Figure 14). αGC also increased IFN-γ production in DOX-treated hearts (Supplemental Figure 15). Consistent with this change, αGC increased phosphorylation of STAT1, ERK, and Akt (Supplemental Figure 16A) and suppressed ratio of Bax to Bcl-2 in DOX-treated hearts (Supplemental Figure 16B).

ERK MEDIATED PROTECTIVE EFFECTS OF IFN-γ AGAINST DOX-INDUCED CARDIOMYOCYTE INJURY. We further investigated the role of IFN-γ and ERK in DOX-induced cardiomyocyte injury. Pretreatment of IFN-γ attenuated decreases in cardiomyocyte survival in response to DOX (Supplemental Figure 17A). Furthermore, beneficial effects of IFN-γ were canceled by both SCH772984 and U0126, ERK inhibitors (Supplemental Figure 17A). U0126 efficiently inhibited phosphorylation of ERK and increased ratio of Bax to Bcl-2 in cardiomyocytes in response to DOX (Supplemental Figure 17B). IFN-γ decreased ratio of Bax to Bcl-2 in cardiomyocytes in response to DOX and these beneficial effects were abolished by U0126 (Supplemental Figure 17B). These data indicate that IFN-γ plays a protective role against DOX-induced cardiomyocyte death through ERK activation.

DISCUSSION

The present study demonstrated that activation of iNKT cells by αGC ameliorated DOX-induced cardiac dysfunction and myocardial apoptosis. These protective effects were mediated by the IFN-γ-STAT1-ERK pathway. Activation of iNKT cells also preserved energy metabolism and redox-related protein levels in DOX-treated hearts. The present study revealed a novel protective mechanism against DOX-induced cardiomyopathy by activation of iNKT cells (Supplemental Figure 18).

Myocardial inflammation is implicated with DOX-induced cardiac dysfunction. In particular, inflammatory cytokines such as IL-1β, IL-6, TNF-α, IL-10, and IFN-γ are known to be intimately involved in pathophysiology of DOX-induced cardiomyopathy.[13-16,26] iNKT cells can produce various cytokines, including IL-4, IL-10, and IFN-γ, and orchestrate tissue inflammation. iNKT cells are known to exert a protective action on cardiac dysfunction by regulating cytokines. Activation of iNKT cells plays a protective role in cardiac remodeling after post-myocardial infarction and ischemia-reperfusion injury by enhancing IL-10 expression.[18,19] In the present study, activation of iNKT cells by αGC ameliorated cardiac dysfunction in DOX-treated hearts (**Figure 2**), which was accompanied by a persistent increase in IFN-γ, but not other cytokines (**Figure 4**). In addition, αGC suppressed apoptosis in DOX-treated hearts (**Figures 3C and 3D**). Importantly, neutralization of IFN-γ by its antibody canceled these protective effects by αGC, suggesting that IFN-γ mediated the protective effects of iNKT cells (**Figure 6**). IFN-γ is

FIGURE 3 αGC Administration Attenuated DOX-Induced Cardiomyocyte Injury and Apoptosis

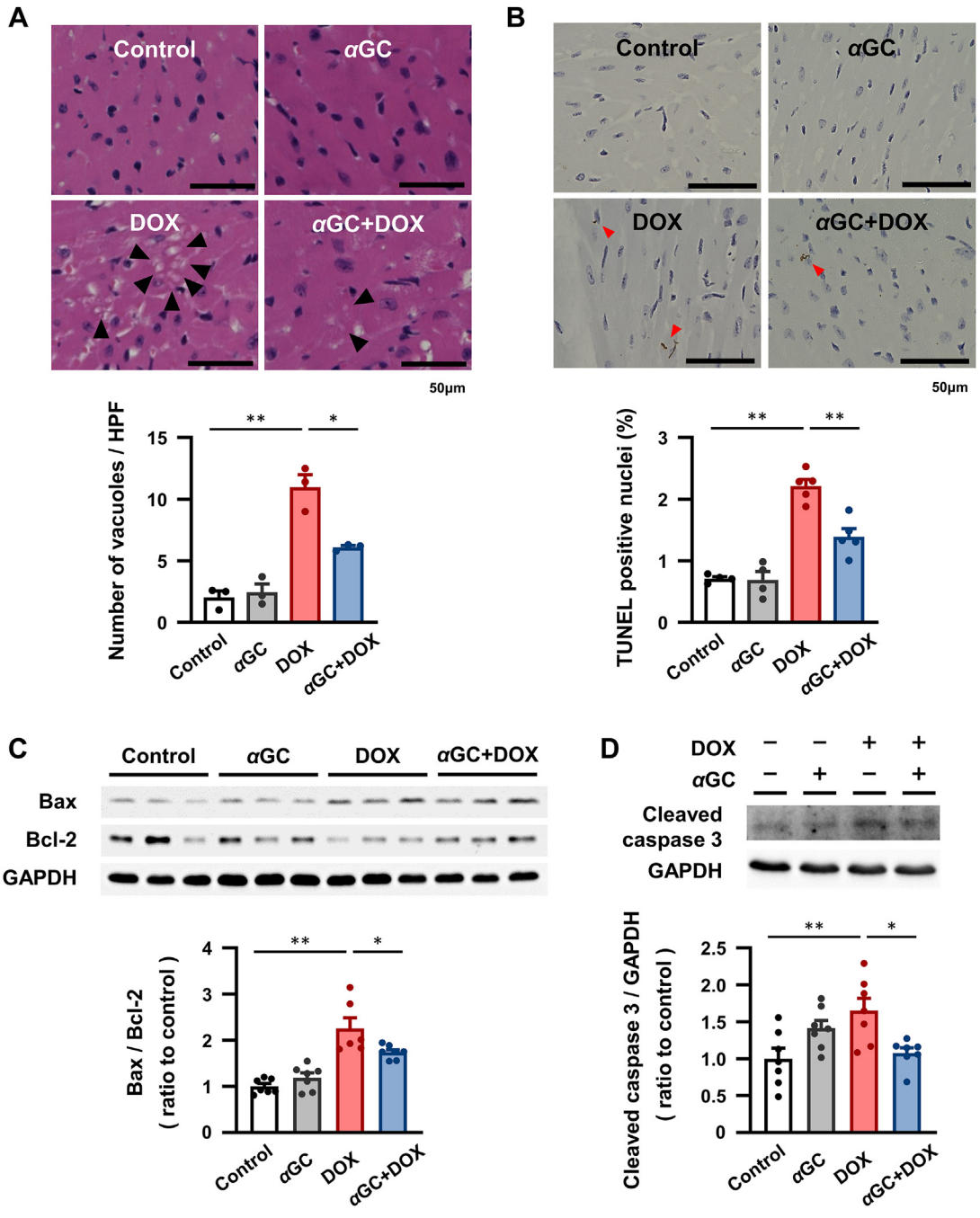

(A) Representative images of hematoxylin and eosin staining and quantification of the number of cytoplasmic vacuolization in the LV of vehicle and αGC-treated mice 14 days after DOX injection (n = 3). **Black arrows** indicate cytoplasmic vacuolization. **(B)** Representative images of terminal deoxynucleotidyl transferase dUTP nick end labeling (TUNEL) staining and quantification of the percentage of TUNEL-positive nuclei in the LV of indicated mice (n = 4–5). **Red arrowheads** indicate TUNEL-positive nuclei. **(C)** Representative immunoblots and quantitative analysis of Bcl-2-associated X protein (Bax) and B cell/CLL lymphoma 2 (Bcl-2) in the LV of indicated mice (n = 7). **(D)** Representative immunoblots and quantitative analysis of cleaved caspase 3 in the LV of indicated mice (n = 7). Data are expressed as mean ± SEM. *$P < 0.05$, **$P < 0.01$: ANOVA with Tukey's post hoc test. HPF = high-powered field; other abbreviations as in Figure 1.

involved in a multitude of processes in innate and adaptive immunity.[27] To date, the role of IFN-γ in cell survival and inflammation is controversial. Yin et al[28] demonstrated that IFN-γ induced apoptosis in tumor cells. IFN-γ disrupts mitochondrial respiration and deteriorates cardiac function in DOX-treated mice.[26] On the other hand, IFN-γ rescued an imbalance of inflammation in lung injury.[29] IFN-γ is necessary for B cell survival in rheumatoid arthritis.[30] IFN-γ is also known to protect cardiac hypertrophy in response to pressure overload and aldosterone infusion.[31] Recently, IFN-γ was reported to regulate immune response and preserve cardiac function post-myocardial infarction.[32] Therefore, the role of IFN-γ might depend on the type of cardiac injury and its severity. Regarding the role of IFN-γ, our results are still inconsistent with the previous study.[26] This discrepancy might be due to different experimental conditions, such as doses and concentrations of DOX and timing of evaluation of cell death and administration of IFN-γ. We here demonstrated that, although IFN-γ is not endogenously involved in pathophysiology of DOX-induced cardiomyopathy, IFN-γ mediated protective effects by reducing myocardial apoptosis in the setting of activation of iNKT cells (**Figure 6**). These findings indicate that the impact of IFN-γ on DOX-induced cardiomyopathy might be stipulated not only by itself but also other factors. Importantly, it must be taken into consideration that our study reveals the protective role of IFN-γ in the setting of activation of NKT cells in vivo. To elucidate the distinct role of IFN-γ in DOX-induced cardiotoxicity, further investigations are needed.

STAT1 mediates IFN-γ stimulation as a downstream of its receptor.[33] MAP kinases and Akt are known to exert protective effects against DOX-induced myocardial apoptosis.[34-36] In the present study, consistent with IFN-γ, αGC increased phosphorylation of STAT1, ERK, and Akt in DOX-treated hearts (**Figure 5**). Importantly, administration of anti-IFN-γ neutralizing antibody canceled phosphorylation of STAT1 and ERK, but not Akt (**Figure 6**), suggesting that STAT1 and ERK mediated the anti-apoptotic effect of iNKT cells as downstream of IFN-γ in DOX-induced cardiomyopathy.

Although TUNEL staining has been used for evaluation of apoptosis in DOX-cardiomyopathy in previous studies,[37-40] it is not specific for apoptosis. Therefore, in addition to Bax/Bcl-2 ratio, we now evaluated cleaved caspase 3 in the heart. DOX treatment increased cleaved caspase 3 and αGC administration attenuated it (**Figure 3D**). Furthermore, anti-IFN-γ antibody canceled a suppressive effect of cleaved caspase 3 by αGC in DOX-induced cardiomyopathy (**Figure 6D**). We also investigated signaling of other types of cell death. Contrary to cleaved caspase 3, DOX treatment or αGC administration did not alter phosphorylation of MLKL, a mediator of necroptosis (Supplemental Figure 2). These findings provide a relevance of apoptosis in pathophysiology of DOX-induced cardiomyopathy and effectiveness of iNKT cell activation.

Cardiomyocyte death, including apoptosis, is intimately involved in energy metabolism and redox. To evaluate the effect of activation of iNKT cells on energy metabolism and redox, we performed mass spectrometric analysis in the present study. Interestingly, activation of iNKT cells preserved 50 proteins related to oxidative phosphorylation, TCA cycle, FAO, and antioxidant capacity in DOX-treated hearts (Supplemental Table 1, Supplemental Figure 8), raising a possibility that activation of iNKT cells decreased myocardial apoptosis by preserving energy metabolism and antioxidant capacity. However, a regulatory mechanism of these proteins still unclear and further investigations regarding relationship between these proteins and the IFN-γ-STAT1-ERK pathway are needed.

Most recently, iNKT cells have been reported to enhance mRNA expressions of arginase 1, a marker of M2 macrophage, and attenuate interstitial fibrosis in DOX-treated hearts.[20] However, in the present study, we could not find an increase in arginase 1 (Supplemental Figure 7) and suppression of interstitial fibrosis (Supplemental Figures 3 and 4) by αGC. This discrepancy of inflammatory response by activation of iNKT cells might be due to different ways of αGC administration. In the study by Obata et al,[20] 0.1 μg/g BW of αGC was administrated twice 4 days before and 3 days after DOX injection. On the other hand, 0.1 μg/g BW of αGC was once administered 7 days before DOX injection in this study. It is known that repeated injection of αGC induces anergy in iNKT cells, leading to decreases in IFN-γ production.[41] Thus, a single administration of αGC is thought to predominantly increase IFN-γ. The effect of iNKT cells might be dependent on the mode of its stimulation. This study also provides proof-of-principle evidence that pretreatment with an iNKT cell activator efficiently prevents DOX-induced cardiomyopathy. Another possible explanation of difference in the effect of iNKT cells in fibrosis is that myocardial fibrosis is not obvious in this study. In fact, DOX-

FIGURE 4 αGC Administration Increased IFN-γ Production in DOX-treated Hearts

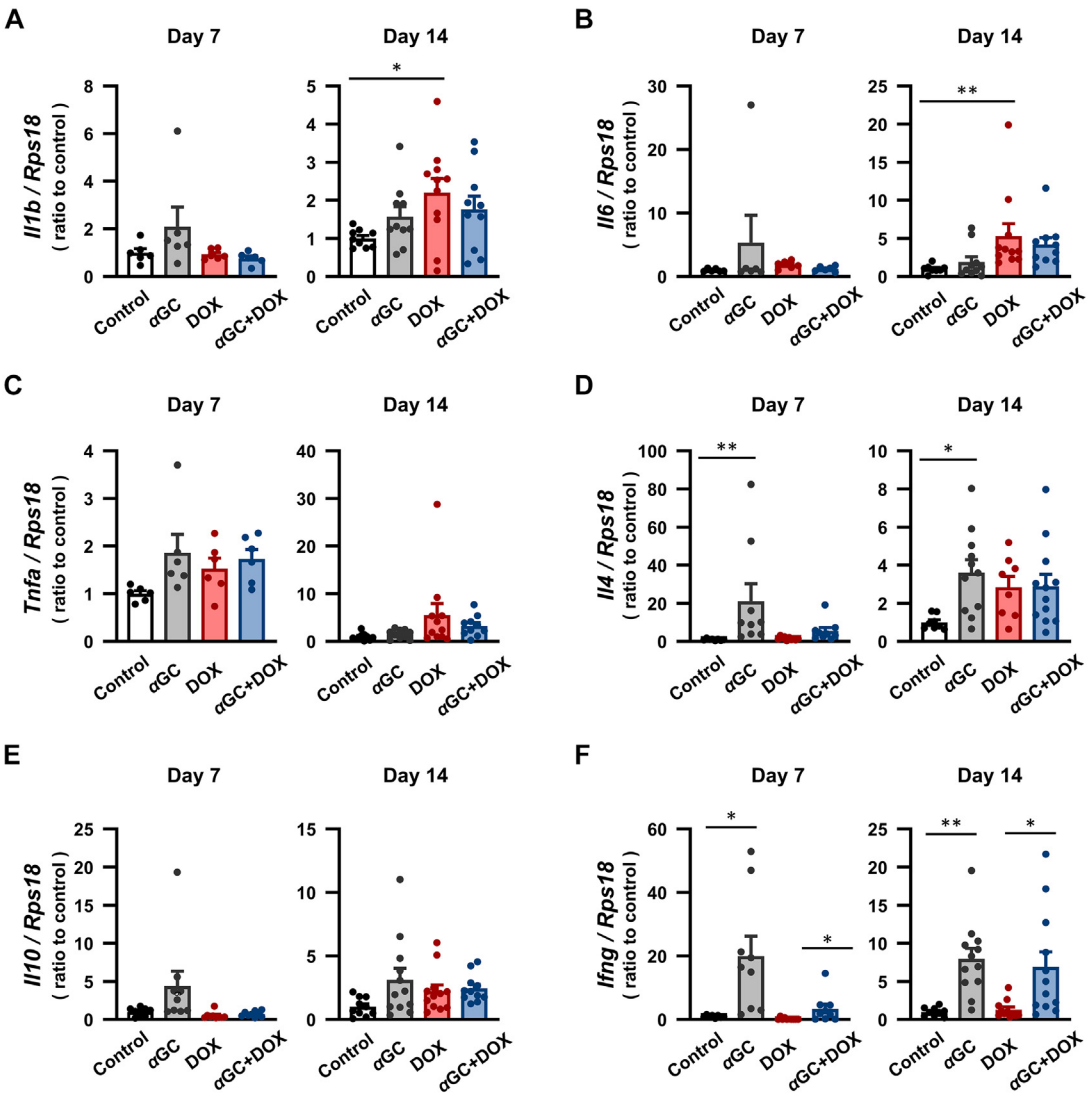

Gene expression of *Il1b* **(A)**, *Il6* **(B)**, *Tnfa* **(C)**, *Il4* **(D)**, *Il10* **(E)**, and *Ifng* **(F)** in the LV of vehicle and αGC-treated mice 7 and 14 days after DOX injection (n = 9–11). Data are expressed as mean ± SEM. *$P < 0.05$, **$P < 0.01$: ANOVA with Tukey's post hoc test or Kruskal-Wallis test. IFN = interferon; other abbreviations as in Figure 1.

induced fibrosis of this study is lower than that of the study by Obata et al[20] (1.5% vs. 4%). Therefore, the antifibrotic effect of iNKT cells might not be proven in our model of DOX-induced cardiomyopathy.

Many animal studies regarding DOX-induced cardiomyopathy have used a model of a single high-dose DOX injection. This model is characterized by not only acute cardiotoxicity but also severe extracardiac phenotypes including BW loss and noncardiac death, resulting in conflicting interpretations with cardiac phenotype and leading to discrepant findings between animal experiment and clinical setting. Recently, a murine model of divided injection of DOX mimicking human DOX-induced cardiomyopathy has been reported, which causes modest but progressive cardiac dysfunction without severe noncardiac effects.[42] We first chose this model to exclude major impact on the extracardiac phenotype in the present study. Furthermore, we investigated 2 additional protocols

FIGURE 5 αGC Administration Increased Phosphorylation of STAT1, ERK, and Akt in DOX-treated Hearts

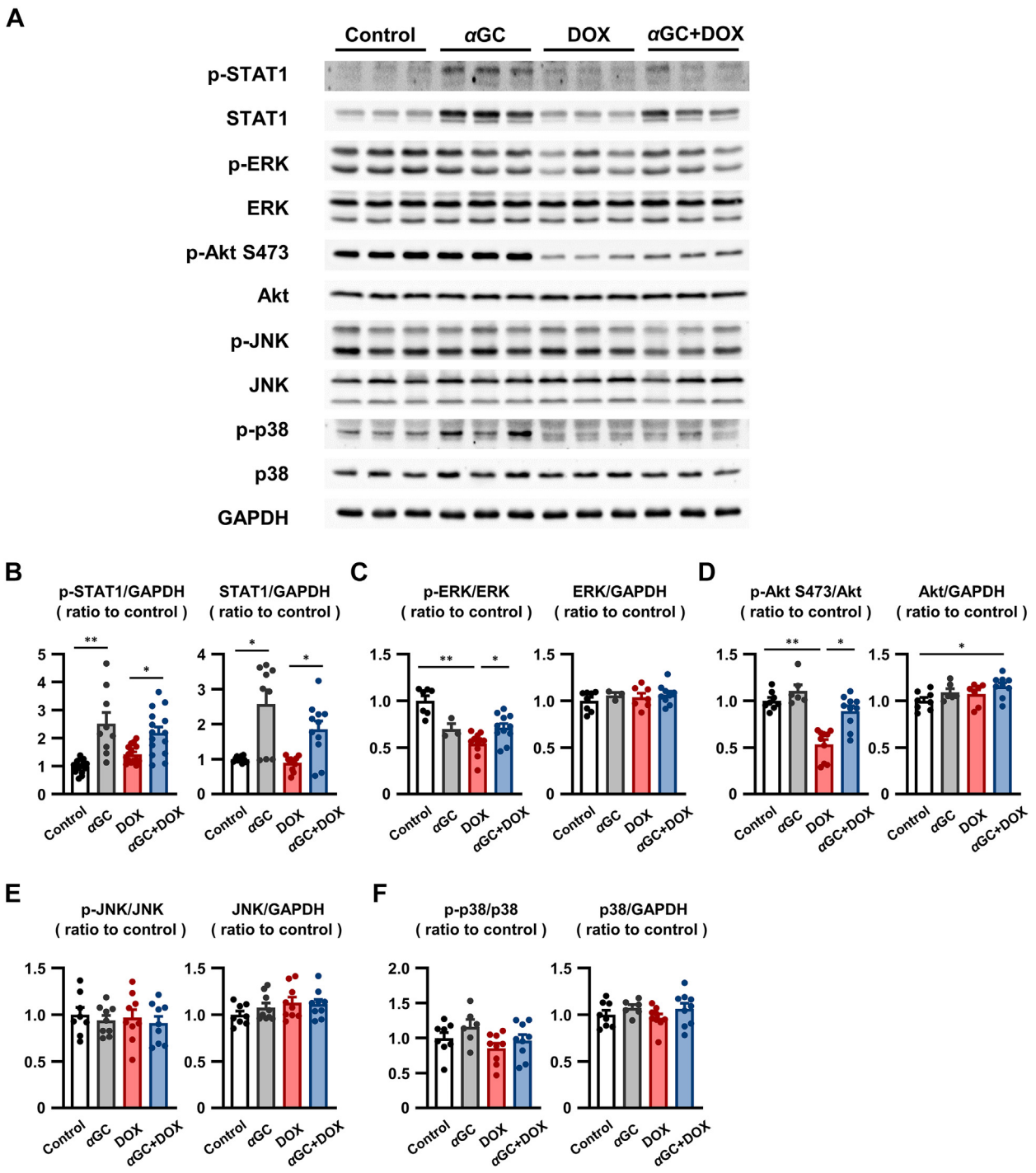

(A) Representative immunoblots of phosphorylation of signal transducers and activators of transcription 1 (STAT1), Akt, extracellular signal-regulated kinase (ERK), c-Jun N-terminal kinase (JNK), and p38 in the LV of vehicle and αGC-treated mice 7 days after DOX injection (n = 8–15). **(B to F)** Quantitative analysis of these signals in the LV of indicated mice. Data are expressed as mean ± SEM. *$P < 0.05$, **$P < 0.01$: ANOVA with Tukey's post hoc test or Kruskal-Wallis test. Abbreviations as in Figure 1.

FIGURE 6 Neutralization of IFN-γ Abolished Protective Effects of αGC on DOX-induced Cardiac Dysfunction and Apoptosis

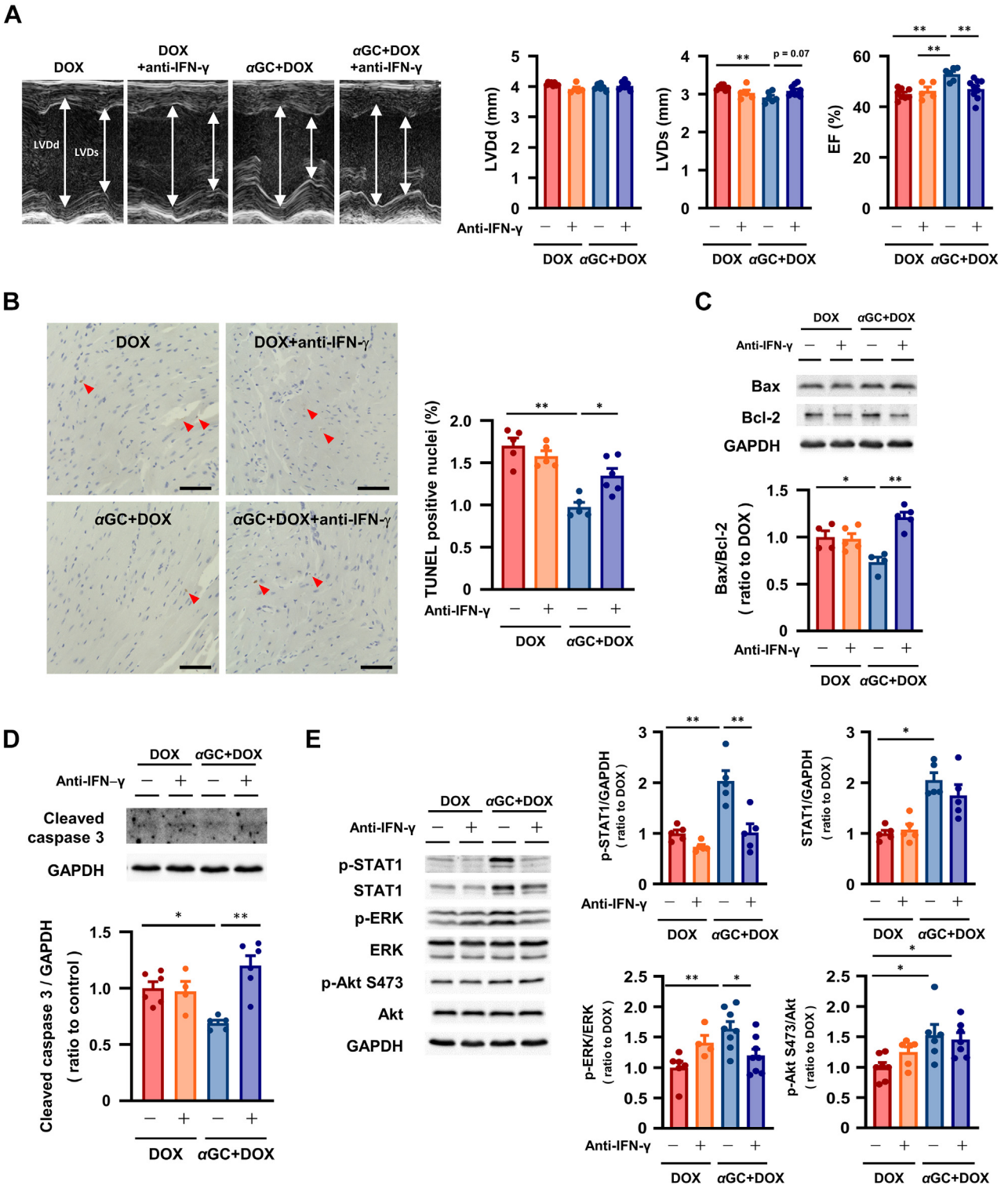

Continued on the next page

(Supplemental Figures 10 and 13). The dosing of DOX induces a variety of pathologies. A high dose of DOX injection in this study induces the extracardiac phenotype to some extent. However, consistent with these previous findings, the present study exhibited that 6 mg/kg ×3 of DOX mildly decreased BW, a marker of extracardiac manifestations. Importantly, the death of mice was observed in the 20 mg/kg of DOX model, but not in the 6 mg/kg ×3 of DOX model. In addition, the extent of cardiac dysfunction was similar between both models. These findings suggest that extracardiac phenotypes in the 20 mg/kg of DOX model are more severe than those in the 6 mg/kg ×3 of DOX model. To investigate the role of iNKT cells in chronic DOX-induced cardiotoxicity, further investigations using a low dose of DOX model are needed.

In this study, pre-administration of αGC (original protocol and additional protocol 2) demonstrated beneficial effects on DOX-induced cardiomyopathy. In these protocols, αGC efficiently increased IFN-γ and phosphorylation of STAT1 and ERK. Therefore, we speculate that the early stimulation of IFN-γ-STAT1-ERK pathway induced by activation of iNKT cells is necessary for the protective role of iNKT cells in DOX-induced cardiomyopathy. Importantly, even in the case of DOX-induced cardiomyopathy with severe extracardiac manifestations, pre-activation of iNKT efficiently enhanced the IFN-γ-STAT1- ERK pathway and attenuated cardiac dysfunction in DOX-treated hearts.

In clinical settings, it is possible to activate iNKT cells before DOX treatment. Furthermore, activation of iNKT cells is applicated as cancer therapy.[43-49] Thus, in the case of combination therapy with DOX, pre-activation of iNKT cells is expected to have a dual benefit of antitumor and cardioprotective effects. We now clearly stated these novelties of our study and discussed a potential clinical relevance of pre-activation of iNKT cell.

There are 3 novel findings in the present study. First, among several cytokines stimulated by iNKT cells, IFN-γ critically mediates a protective effect of iNKT cells via the STAT1-ERK pathway. Second, activation of iNKT cells attenuated abnormalities of protein profiles regarding energy metabolism and antioxidant capacity. Finally, pretreatment of iNKT cell is needed to exert its protective effect against DOX-induced cardiomyopathy.

CONCLUSIONS

Activation of iNKT cells by αGC plays a protective role against DOX-induced cardiomyopathy via IFN-γ-STAT1-ERK pathway. Therapies designed to activate iNKT cells might be beneficial to protect the heart from DOX-induced injury.

ACKNOWLEDGMENTS The authors are grateful to M. Sato and A. Hanada for technical support. They also appreciate the technical assistance from the Research Support Center, Faculty of Medical Sciences, Kyushu University.

FUNDING SUPPORT AND AUTHOR DISCLOSURES

This work was supported by the Japan Society for the Promotion of Science (JSPS) KAKENHI (Grant Nos. JP19K22622, JP19H03655, 21K19485, 21K08082, and 22H03070) and Japan Agency for Medical Research and Development (AMED) (Grant Nos. 20ek0109339h0003). Dr Tsutsui has received personal fees from Merck Sharp and Dohme, Astellas, Pfizer, Bristol-Myers Squibb, Otsuka Pharmaceutical, Daiichi-Sankyo, Mitsubishi Tanabe Pharma, Nippon Boehringer Ingelheim, Takeda Pharmaceutical, Bayer Yakuhin, Novartis Pharma, Kowa Pharmaceutical, Teijin Pharma, Medical Review Co, and the *Japanese Journal of Clinical Medicine*; nonfinancial support from Actelion Pharmaceuticals, Japan Tobacco Inc, Mitsubishi Tanabe Pharma, Nippon Boehringer Ingelheim, Daiichi-Sankyo, IQVIA Services Japan, and Omron Healthcare Co; grants from Astellas, Novartis Pharma, Daiichi-Sankyo, Takeda Pharmaceutical, Mitsubishi Tanabe Pharma, Teijin Pharma, and Merck Sharp and Dohme, outside the submitted work. All other authors have reported that they have no relationships relevant to the contents of this paper to disclose.

ADDRESS FOR CORRESPONDENCE: Dr Shouji Matsushima, Department of Cardiovascular Medicine, Faculty of Medical Sciences, Kyushu University, 3-1-1 Maidashi, Higashi-ku, Fukuoka 812-8582, Japan. E-mail: matsushima.shoji.056@m.kyushu-u.ac.jp.

FIGURE 6 Continued

(A) Representative echocardiographic images and parameters such as LVDd, LVDs, and ejection fraction (EF) in DOX- and αGC + DOX-treated mice with or without anti-IFN-γ antibody (n = 5–9). **(B)** Representative images of TUNEL staining and quantification of the percentage of TUNEL-positive nuclei in the LV of indicated mice (n = 5). **Red arrowheads** indicate TUNEL-positive nuclei. **(C)** Representative immunoblots and quantitative analysis of Bax and Bcl-2 in the LV of indicated mice 8 days after DOX treatment (n = 5). **(D)** Representative immunoblots and quantitative analysis of cleaved caspase 3 in the LV of indicated mice 14 days after DOX treatment (n = 4–6). **(E)** Representative immunoblots and quantitative analysis of phosphorylation of STAT1, ERK, and Akt in the LV of indicated mice 8 days after DOX treatment (n = 6–8). Data are expressed as mean ± SEM. $*P < 0.05$, $**P < 0.01$: ANOVA with Tukey's post hoc test or Kruskal-Wallis test. Abbreviations as in Figures 1 to 5.

PERSPECTIVES

COMPETENCY IN MEDICAL KNOWLEDGE: Myocardial inflammation and disturbance of inflammatory cytokines are intimately involved in DOX-induced cardiomyopathy. iNKT cells are known to orchestrate inflammatory cytokines and regulate myocardial inflammation in the cardiovascular system. However, the role of iNKT cells has not been fully determined in this disease. We here demonstrated that activation of iNKT cells by αGC attenuated DOX-induced cardiomyocyte death and cardiac dysfunction via the IFN-γ-STAT1-ERK pathway.

TRANSLATIONAL OUTLOOK: We here revealed the protective role of iNKT cells in DOX-induced cardiomyopathy and its molecular mechanisms in mice. Activation of iNKT cells by cell therapy such as αGC-pulsed antigen presenting cells has been shown to be beneficial in patients with neck and head cancer. Our findings support clinical translation of activation of iNKT cells as a therapeutic strategy against DOX-induced cardiomyopathy.

REFERENCES

1. Barrett-Lee PJ, Dixon JM, Farrell C, et al. Expert opinion on the use of anthracyclines in patients with advanced breast cancer at cardiac risk. *Ann Oncol*. 2009;20:816–827.

2. Felker GM, Thompson RE, Hare JM, et al. Underlying causes and long-term survival in patients with initially unexplained cardiomyopathy. *N Engl J Med*. 2000;342:1077–1084.

3. Kotamraju S, Konorev EA, Joseph J, Kalyanaraman B. Doxorubicin-induced apoptosis in endothelial cells and cardiomyocytes is ameliorated by nitrone spin traps and ebselen. Role of reactive oxygen and nitrogen species. *J Biol Chem*. 2000;275:33585–33592.

4. Prathumsap N, Shinlapawittayatorn K, Chattipakorn SC, Chattipakorn N. Effects of doxorubicin on the heart: from molecular mechanisms to intervention strategies. *Eur J Pharmacol*. 2020;866:172818.

5. Zhao Y, Sun J, Zhang W, et al. Follistatin-like 1 protects against doxorubicin-induced cardiomyopathy through upregulation of Nrf2. *Oxid Med Cell Longev*. 2020;2020:3598715.

6. Zhang S, Liu X, Bawa-Khalfe T, et al. Identification of the molecular basis of doxorubicin-induced cardiotoxicity. *Nat Med*. 2012;18:1639–1642.

7. Ichikawa Y, Ghanefar M, Bayeva M, et al. Cardiotoxicity of doxorubicin is mediated through mitochondrial iron accumulation. *J Clin Invest*. 2014;124:617–630.

8. Carvalho RA, Sousa RP, Cadete VJ, et al. Metabolic remodeling associated with subchronic doxorubicin cardiomyopathy. *Toxicology*. 2010;270:92–98.

9. Rahmatollahi M, Baram SM, Rahimian R, Saeedi Saravi SS, Dehpour AR. Peroxisome proliferator-activated receptor-alpha inhibition protects against doxorubicin-induced cardiotoxicity in mice. *Cardiovasc Toxicol*. 2016;16:244–250.

10. Abdullah CS, Alam S, Aishwarya R, et al. Doxorubicin-induced cardiomyopathy associated with inhibition of autophagic degradation process and defects in mitochondrial respiration. *Sci Rep*. 2019;9:2002.

11. Hrelia S, Fiorentini D, Maraldi T, et al. Doxorubicin induces early lipid peroxidation associated with changes in glucose transport in cultured cardiomyocytes. *Biochim Biophys Acta*. 2002;1567:150–156.

12. Maejima Y, Adachi S, Morikawa K, Ito H, Isobe M. Nitric oxide inhibits myocardial apoptosis by preventing caspase-3 activity via S-nitrosylation. *J Mol Cell Cardiol*. 2005;38:163–174.

13. Sauter KA, Wood LJ, Wong J, Iordanov M, Magun BE. Doxorubicin and daunorubicin induce processing and release of interleukin-1beta through activation of the NLRP3 inflammasome. *Cancer Biol Ther*. 2011;11:1008–1016.

14. Guo RM, Xu WM, Lin JC, et al. Activation of the p38 MAPK/NF-kappaB pathway contributes to doxorubicin-induced inflammation and cytotoxicity in H9c2 cardiac cells. *Mol Med Rep*. 2013;8:603–608.

15. Riad A, Bien S, Gratz M, et al. Toll-like receptor-4 deficiency attenuates doxorubicin-induced cardiomyopathy in mice. *Eur J Heart Fail*. 2008;10:233–243.

16. Singla DK, Johnson TA, Tavakoli Dargani Z. Exosome treatment enhances anti-inflammatory M2 macrophages and reduces inflammation-induced pyroptosis in doxorubicin-induced cardiomyopathy. *Cells*. 2019;8:1224.

17. Matsuda JL, Mallevaey T, Scott-Browne J, Gapin L. CD1d-restricted iNKT cells, the 'Swiss-Army knife' of the immune system. *Curr Opinion Immunol*. 2008;20:358–368.

18. Sobirin MA, Kinugawa S, Takahashi M, et al. Activation of natural killer T cells ameliorates postinfarct cardiac remodeling and failure in mice. *Circ Res*. 2012;111:1037–1047.

19. Homma T, Kinugawa S, Takahashi M, et al. Activation of invariant natural killer T cells by alpha-galactosylceramide ameliorates myocardial ischemia/reperfusion injury in mice. *J Mol Cell Cardiol*. 2013;62:179–188.

20. Obata Y, Ishimori N, Saito A, et al. Activation of invariant natural killer T cells by alpha-galactosylceramide ameliorates doxorubicin-induced cardiotoxicity in mice. *Eur J Prev Cardiol*. 2020;27:2358–2361.

21. Ikeda S, Matsushima S, Okabe K, et al. Blockade of L-type Ca(2+) channel attenuates doxorubicin-induced cardiomyopathy via suppression of CaMKII-NF-kappaB pathway. *Sci Rep*. 2019;9:9850.

22. Ikeda M, Ide T, Fujino T, et al. The Akt-mTOR axis is a pivotal regulator of eccentric hypertrophy during volume overload. *Sci Rep*. 2015;5:15881.

23. Matsushima S, Ide T, Yamato M, et al. Overexpression of mitochondrial peroxiredoxin-3 prevents left ventricular remodeling and failure after myocardial infarction in mice. *Circulation*. 2006;113:1779–1786.

24. Yamamoto S, Yang G, Zablocki D, et al. Activation of Mst1 causes dilated cardiomyopathy by stimulating apoptosis without compensatory ventricular myocyte hypertrophy. *J Clin Invest*. 2003;111:1463–1474.

25. Zhai P, Yamamoto M, Galeotti J, et al. Cardiac-specific overexpression of AT1 receptor mutant lacking G alpha q/G alpha i coupling causes hypertrophy and bradycardia in transgenic mice. *J Clin Invest*. 2005;115:3045–3056.

26. Ni C, Ma P, Wang R, et al. Doxorubicin-induced cardiotoxicity involves IFNgamma-mediated metabolic reprogramming in cardiomyocytes. *J Pathol*. 2019;247:320–332.

27. Schroder K, Hertzog PJ, Ravasi T, Hume DA. Interferon-gamma: an overview of signals, mechanisms and functions. *J Leukoc Biol*. 2004;75:163–189.

28. Yin H, Jiang Z, Wang S, Zhang P. IFN-gamma restores the impaired function of RNase L and induces mitochondria-mediated apoptosis in lung cancer. *Cell Death Dis*. 2019;10:642.

29. Eldredge LC, Creasy RS, Tanaka S, Lai JF, Ziegler SF. Imbalance of Ly-6C(hi) and Ly-6C(lo) monocytes/macrophages worsens hyperoxia-induced lung injury and is rescued by IFN-gamma. *J Immunol*. 2019;202:2772–2781.

30. Lowin T, Anssar TM, Bauml M, Classen T, Schneider M, Pongratz G. Positive and negative cooperativity of TNF and Interferon-gamma in regulating synovial fibroblast function and B cell survival in fibroblast/B cell co-cultures. *Sci Rep*. 2020;10:780.

31. Kimura A, Ishida Y, Furuta M, et al. Protective roles of interferon-gamma in cardiac hypertrophy induced by sustained pressure overload. *J Am Heart Assoc*. 2018;7:e008145.

32. Finger S, Knorr M, Molitor M, et al. A sequential interferon gamma directed chemotactic cellular immune response determines survival and cardiac function post-myocardial infarction. *Cardiovasc Res*. 2019;115:1907–1917.

33. DaFonseca CJ, Shu F, Zhang JJ. Identification of two residues in MCM5 critical for the assembly of MCM complexes and Stat1-mediated transcription activation in response to IFN-gamma. *Proc Natl Acad Sci U S A*. 2001;98:3034–3039.

34. Lou H, Danelisen I, Singal PK. Involvement of mitogen-activated protein kinases in adriamycin-induced cardiomyopathy. *Am J Physiol Heart Circ Physiol*. 2005;288:H1925–H1930.

35. Xiang P, Deng HY, Li K, et al. Dexrazoxane protects against doxorubicin-induced cardiomyopathy: upregulation of Akt and Erk phosphorylation in a rat model. *Cancer Chemother Pharmacol*. 2009;63:343–349.

36. Yu X, Cui L, Zhang Z, Zhao Q, Li S. alpha-Linolenic acid attenuates doxorubicin-induced cardiotoxicity in rats through suppression of oxidative stress and apoptosis. *Acta Biochim Biophys Sin (Shanghai)*. 2013;45:817–826.

37. Nozaki N, Shishido T, Takeishi Y, Kubota I. Modulation of doxorubicin-induced cardiac dysfunction in toll-like receptor-2-knockout mice. *Circulation*. 2004;110:2869–2874.

38. Neilan TG, Blake SL, Ichinose F, et al. Disruption of nitric oxide synthase 3 protects against the cardiac injury, dysfunction, and mortality induced by doxorubicin. *Circulation*. 2007;116:506–514.

39. Tadokoro T, Ikeda M, Ide T, et al. Mitochondria-dependent ferroptosis plays a pivotal role in doxorubicin cardiotoxicity. *JCI Insight*. 2020;5:e132747.

40. Li HR, Wang C, Sun P, Liu DD, Du GQ, Tian JW. Melatonin attenuates doxorubicin-induced cardiotoxicity through preservation of YAP expression. *J Cell Mol Med*. 2020;24:3634–3646.

41. Kojo S, Elly C, Harada Y, Langdon WY, Kronenberg M, Liu YC. Mechanisms of NKT cell anergy induction involve Cbl-b-promoted monoubiquitination of CARMA1. *Proc Natl Acad Sci U S A*. 2009;106:17847–17851.

42. Hull TD, Boddu R, Guo L, et al. Heme oxygenase-1 regulates mitochondrial quality control in the heart. *JCI Insight*. 2016;1:e85817.

43. Kawano T, Nakayama T, Kamada N, et al. Antitumor cytotoxicity mediated by ligand-activated human V alpha24 NKT cells. *Cancer Res*. 1999;59:5102–5105.

44. Seino K, Motohashi S, Fujisawa T, Nakayama T, Taniguchi M. Natural killer T cell-mediated antitumor immune responses and their clinical applications. *Cancer Sci*. 2006;97:807–812.

45. Motohashi S, Nakayama T. Clinical applications of natural killer T cell-based immunotherapy for cancer. *Cancer Sci*. 2008;99:638–645.

46. Motohashi S, Okamoto Y, Yoshino I, Nakayama T. Anti-tumor immune responses induced by iNKT cell-based immunotherapy for lung cancer and head and neck cancer. *Clin Immunol*. 2011;140:167–176.

47. Horinaka A, Sakurai D, Ihara F, et al. Invariant NKT cells are resistant to circulating CD15+ myeloid-derived suppressor cells in patients with head and neck cancer. *Cancer Sci*. 2016;107:207–216.

48. Ishibashi F, Sakairi Y, Iwata T, et al. A phase I study of loco-regional immunotherapy by transbronchial injection of alpha-galactosylceramide-pulsed antigen presenting cells in patients with lung cancer. *Clin Immunol*. 2020;215:108457.

49. Hara A, Koyama-Nasu R, Takami M, et al. CD1d expression in glioblastoma is a promising target for NKT cell-based cancer immunotherapy. *Cancer Immunol Immunother*. 2021;70:1239–1254.

KEY WORDS apoptosis, cardiomyopathy, doxorubicin, interferon-gamma, natural killer T cells

APPENDIX For a supplemental Methods section, and supplemental, figures, and a table, please see the online version of this paper.